

NO-A180 037

THE HUECKEL MODEL FOR SMALL METAL CLUSTERS 3 ANION
STRUCTURES AND HMO (HU) (U) STATE UNIV OF NEW YORK AT
BUFFALO DEPT OF CHEMISTRY D M LINDSAY ET AL APR 87

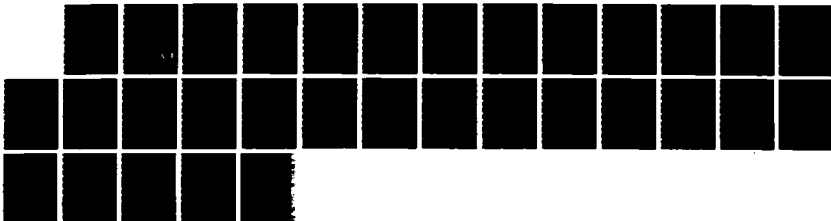
1/1

UNCLASSIFIED

UBUFFALO/DC/87/TR-36 N00014-86-K-0043

F/G 20/5

NL



1.0	1.2
1.1	1.3
1.25	1.4
	1.5
	1.6
	1.8
	2.0
	2.2
	2.3

12

AD-A180 037

OFFICE OF NAVAL RESEARCH

Contract N00014-86-K-0043

R & T Code 413f0001--01

TECHNICAL REPORT No. 36

The Huckel Model for Small Metal Clusters. III. Anion Structures
and ~~HMO~~ Electron Affinities

by

D. M. Lindsay, Lin Chu, Youqi Wang and Thomas F. George

Prepared for Publication

in

Journal of Chemical Physics

Departments of Chemistry and Physics
State University of New York at Buffalo
Buffalo, New York 14260

April 1987

Reproduction in whole or in part is permitted for any purpose of the
United States Government.

This document has been approved for public release and sale;
its distribution is unlimited

DTIC
ELECTE
MAY 07 1987
S E D

REPORT DOCUMENTATION PAGE

1a. REPORT SECURITY CLASSIFICATION Unclassified			1b. RESTRICTIVE MARKINGS		
2a. SECURITY CLASSIFICATION AUTHORITY			3. DISTRIBUTION/AVAILABILITY OF REPORT Approved for public release; distribution unlimited		
2b. DECLASSIFICATION/DOWNGRADING SCHEDULE					
4. PERFORMING ORGANIZATION REPORT NUMBER(S) UBUFFALO/DC/87/TR-36			5. MONITORING ORGANIZATION REPORT NUMBER(S)		
6a. NAME OF PERFORMING ORGANIZATION Depts. Chemistry & Physics State University of New York		6b. OFFICE SYMBOL (If applicable)	7a. NAME OF MONITORING ORGANIZATION		
6c. ADDRESS (City, State and ZIP Code) Fronczak Hall, Amherst Campus Buffalo, New York 14260			7b. ADDRESS (City, State and ZIP Code)		
8a. NAME OF FUNDING/SPONSORING ORGANIZATION Office of Naval Research		8b. OFFICE SYMBOL (If applicable)	9. PROCUREMENT INSTRUMENT IDENTIFICATION NUMBER Contract N00014-86-K-0043		
8c. ADDRESS (City, State and ZIP Code) Chemistry Program 800 N. Quincy Street Arlington, Virginia 22217			10. SOURCE OF FUNDING NOS.		
			PROGRAM ELEMENT NO.	PROJECT NO.	TASK NO.
			WORK UNIT NO.		
11. TITLE The Hückel Model for Small Metal Clusters. III. Anion Structures and HMO Electron Affinities.					
12. PERSONAL AUTHOR(S) D. M. Lindsay, L. Chu, Y. Wang and Thomas F. George					
13a. TYPE OF REPORT		13b. TIME COVERED FROM _____ TO _____		14. DATE OF REPORT (Yr., Mo., Day) April 1987	15. PAGE COUNT 32
16. SUPPLEMENTARY NOTATION Prepared for Publication in Journal of Chemical Physics					
17. COSATI CODES			18. SUBJECT TERMS (Continue on reverse if necessary and identify by block number)		
FIELD	GROUP	SUB. GR.	ALKALI-LIKE METAL CLUSTERS,	HMO ELECTRON AFFINITIES,	
			ANIONS,	COMPARE WITH EXPERIMENTS,	
			HÜCKEL MODEL,	SMALL COPPER CLUSTERS,	
19. ABSTRACT (Continue on reverse if necessary and identify by block number) The most stable structures for the alkali-like clusters $M_3^{\eta-}-M_9^{\eta-}$ are calculated within the framework of the simple Hückel model. The Hückel geometries are, on average, slightly "less compact" than those of the neutral and cation clusters, a phenomenon which may be related to the additional electronic kinetic energy of the anions. Cluster compactness is quantified by an estimation of "soft sphere" volumes, which also allows for a comparison of classical and experimental polarizabilities. The Hückel model gives electron affinities which compare favorably with the experimental results for $Cu_2^{\eta-}-Cu_9^{\eta-}$. To our knowledge, the Hückel results in this paper represent the first systematic search for the stable structures of small alkali-like anion clusters.					
20. DISTRIBUTION/AVAILABILITY OF ABSTRACT UNCLASSIFIED/UNLIMITED <input checked="" type="checkbox"/> SAME AS RPT. <input checked="" type="checkbox"/> DTIC USERS <input type="checkbox"/>			21. ABSTRACT SECURITY CLASSIFICATION Unclassified		
22a. NAME OF RESPONSIBLE INDIVIDUAL Dr. David L. Nelson			22b. TELEPHONE NUMBER (Include Area Code) (202) 696-4410	22c. OFFICE SYMBOL	

**THE HÜCKEL MODEL FOR SMALL METAL CLUSTERS. III.
ANION STRUCTURES AND HMO ELECTRON AFFINITIES.**

D. M. Lindsay and Lin Chu
Department of Chemistry
City University of New York, The City College
New York, New York 10031

Youqi Wang
Department of Chemistry
California Institute of Technology
Pasadena, California 91125

Thomas F. George
Departments of Chemistry and Physics & Astronomy
State University of New York at Buffalo
Buffalo, New York 14260

Accession For	
NTIS GRA&I	<input checked="" type="checkbox"/>
DTIC TAB	<input type="checkbox"/>
Unannounced	<input type="checkbox"/>
Justification	
By _____	
Distribution/	
Availability Codes	
Dist	Avail and/or Special
A-1	



ABSTRACT

The *most stable* structures for the alkali-like clusters, $M_3^- - M_8^-$, are calculated within the framework of the simple Hückel model. The Hückel geometries are, on average, slightly "less compact" than those of the neutral and cation clusters, a phenomenon which may be related to the additional electronic kinetic energy of the anions. Cluster compactness is quantified by an estimation of "soft sphere" volumes, which also allows for a comparison of classical and experimental polarizabilities. The Hückel model gives electron affinities which compare favorably with the experimental results for $Cu_2 - Cu_8$. To our knowledge, the Hückel results in this paper represent the first *systematic* search for the stable structures of small alkali-like *anion* clusters.

I. INTRODUCTION

In previous work,^{1,2} we reported Hückel molecular orbital (HMO) structures for alkali-like clusters M_n and M_n^+ with $2 \leq n \leq 9$. The *most stable* Hückel geometries were found to be the same (except for M_5^+ and M_6^+) as those predicted by local spin density (LSD)^{3,4} and configuration interaction (CI)^{5,6} calculations for the alkali metals. The Hückel results are also in accord with the experimentally determined structures of the ground state Group IA^{7,8} and Group IB⁹⁻¹¹ trimer and heptamer molecules. Moreover, when specialized to neutral Na clusters, the relative agreement between HMO and LSD³ atomization energies was less than 4%. For cation clusters, the discrepancy between LSD atomization energies and the Hückel values, modified by the addition of a classical charge term, was (on average) only 2%. Hückel ionization potentials (IP's) give a good fit to the measured IP's for both Na_n and K_n , reproducing both the observed odd < even alternation in this parameter and the average, or classical, decrease towards the bulk work function.

Recently, two groups have made extensive electron affinity (EA) measurements on copper clusters.^{16,17} These data show an odd > even alternation superimposed on a gradual increase towards the bulk work function. In this paper, we present simple Hückel calculations for alkali-like anion clusters M_n^- . As in the earlier analysis of M_n and M_n^+ , we determine the most stable anion structures amongst *all possible* Hückel bonding arrangements. Cluster atomization energies are computed by combining HMO binding energies with a classical charge-correlation term similar to that introduced in Ref. 2. Using these energies plus the neutral cluster results of Ref. 3, the Hückel model gives electron affinities which reproduce quite well the experimental data for Cu_7-Cu_8 .

II. CLUSTER ANIONS

The HMO stability of an n atom (neutral or ionic) metal cluster is determined by the eigenvalues (ϵ_i) of the Hückel matrix whose elements are given by ($1 \leq i \neq j \leq n$):

$$H_{ij} = \alpha \quad (1)$$
$$H_{ij} = \begin{cases} -\beta, & \text{if } i \text{ is bonded to } j \\ 0, & \text{otherwise} \end{cases}$$

In Eq. (1), α and β denote the empirical Hückel Coulomb and resonance integrals, respectively.

For the anionic clusters of interest here, the binding energy of a particular bonding arrangement is

$$E^-(n) = (n+1)\alpha + \sum_i n_i \epsilon_i^- \quad (2)$$
$$n+1 = \sum_i n_i$$

where the summations extend over all occupied ($n_i = 2$) or partially occupied ($n_i = 1$) molecular orbitals. It is most convenient to choose energy units for which $\alpha = 0$ and $\beta = 1$. As in two previous studies,^{1,2} we term these "Hückel units", abbreviated to hu.

In order to determine relative HMO stabilities, it is necessary to diagonalize the Hückel matrices for all the *physically realizable* bonding arrangements of a particular sized cluster. As described in detail in Ref.1, this procedure is facilitated by using certain concepts from Graph Theory. Briefly, there is a 1-1 correspondence between the Hückel matrix of an n atom cluster containing q bonds and the adjacency matrix of a simple (n,q) graph. It is relatively straightforward to generate all (n,q) graphs and then to eliminate those that are isomorphic by making comparisons with "standard graphs" stored in the form of their incidence matrices. The validity of this procedure can be checked by Polya's

Enumeration Theorem, which can predict the number of distinct and also connected (n,q) graphs. The graphs may be arranged in order of decreasing stability, as defined by Eq.(2), eliminating those for which no hard sphere packing arrangement exists. In order to accomplish this last step, it was mathematically convenient (and physically plausible) to require a maximum separation between all non-bonded atoms.

Figure 1 shows the structures found for the most stable anions, M_3^- - M_8^- . The corresponding binding energies are given in column 3 of Table 1. While the geometries of M_4^- and M_7^- are the same as those found for the neutral (and cation) tetramer and heptamer,¹ this is not the case for the remaining anions. Thus, linear M_3^- is 0.8 hu more stable than the D_{3h} arrangement favoured by the neutral and cationic species. It is interesting to note that SCF-CI calculations on Li_3^{18} and Ag_3^{19} also find that the anion geometry is $D_{\infty h}$. Two isoergic structures were found for M_5^- . One of these, the square pyramid as shown in Fig.1c, is (by 0.2 hu) the second most stable HMO neutral.¹ While the "less compact" ²⁰ D_{5h} structure is as stable as the square pyramid for M_5^- , it is 0.6 hu less stable for neutral M_5 . The most stable M_6^- structure, Fig.1d, has very low symmetry and is best described as a capped, distorted square pyramid. The second (by only 0.02 hu) most stable M_6^- is much more compact. The structure shown in Fig.1e may be derived from M_7^- (Fig.1f) by removing one ring atom. The most stable M_6^- cluster is very similar to that found for neutral M_6 .¹ The Fig.1g structure differs from that of Ref.1 by the breaking of a single bond, which lowers the anion energy by 0.1 hu but raises that of the neutral octamer by 0.4 hu.

Aside from M_3^- (we exclude the dimer), there have been no *ab-initio* calculations on the Group IA and IB cluster anions. The stabilities of a few *selected structures* for silver cluster anions up to about Ag_{20}^- have been explored by semi-empirical methods, mainly as an aid to interpreting electron affinity and ionization potential data.^{21,22} To our knowledge, the HMO results presented here represent the first comprehensive attempt to understand the structures of small anion clusters.

III. ELECTRON AFFINITIES

The thermodynamic EA of a cluster is given by

$$EA(n) = EA(1) + \Delta E^-(n) - \Delta E^0(n) \quad (3)$$

where $\Delta E^0(n)$ and $\Delta E^-(n)$ are the atomization energies of the neutral and anion cluster, respectively. The neutral cluster atomization energy is the endoergicity for

$$M_n = nM \quad (4)$$

and, in the HMO model, is numerically equal to the neutral cluster binding energy, $E^0(n)$ in hu. Table I gives $E^0(n)$ obtained from Ref. 1. Table I also gives $\Delta E^0(n)$ for copper clusters. These data pertain to $\langle\beta\rangle = 1.06 \pm 0.07$ eV, which is an average obtained²³ from the experimental cohesive energy of the bulk²⁴ plus the dimer and trimer atomization energies.²⁵

The anion atomization energy is the energy change for the process

$$M_n^- = (n-1)M + M^- \quad (5)$$

and this is composed of a bond breaking term, numerically equal to $E^-(n)$ expressed in hu, plus an electrostatic term, $\xi^-(n)$. The latter represents the change in self-energy arising from the relocalization of negative charge implied in Eq. (5). Similarly to the previously discussed cation example,² we write $\xi^-(n)$ as

$$\xi^-(n) = 5/8 e^2 \{1/r_1 - 1/r_n\} \quad (6)$$

where e is the electron charge and r_n is the radius of an n atom anion cluster. In terms of an atomic radius, here taken to be the Wigner-Seitz radius (r_s),

$$r_n = r_s(n^{1/3} + \epsilon^-) \quad (7)$$

where ϵ^- is a "charge spillout" parameter ^{2,17} for *anions*. We adopt $\epsilon^- \sim 1$, which is in agreement with the atom-bulk interpolation discussed in the next paragraph. The choice $\epsilon^- \sim 1$ is also in accord with the expected relative (compared to the neutral and cation) diffusiveness of an anion cluster, but is somewhat larger than that used in Ref.17.

The numerical factor of 5/8 in Eq. (6) is chosen to give agreement with the expression for the EA of a classical, conducting drop ^{26,27}

$$EA(n) = W(\infty) - \frac{5}{8} \frac{e^2}{r_n} \quad (8)$$

where $W(\infty)$ is the work function of the bulk metal.²⁸ The correspondence between these two viewpoints may be seen as follows. For a "classical cluster", the bond energies of the neutral and anion species are identical, so that

$$EA(n) = EA(1) + \xi^-(n) \quad (9)$$

For this situation, Eq. (6) together with the identity $EA(\infty) = W(\infty)$, leads directly to Eq.(8).

For $\epsilon^- = 1$, Eqs. (7) and (8) imply

$$W(\infty) - EA(1) = \frac{5e^2}{16r_s} \quad (10)$$

Table II makes a comparison between $W(\infty) - EA(1)$ and $\frac{5e^2}{16r_s}$ for both the Group IA and Group IB elements.²⁹ Except for Li, the average deviation between these two parameters is less than 5%.

As in the case of M_n^+ , we use *modified* simple Hückel atomization energies for the anions. These employ the HMO energies, column 2 of Table I, plus the charge-correlation term, Eq. (6) with $r_n = r_s(n^{1/3} + 1)$. Column 5 of Table I gives $\Delta E^-(n)/n$ for Cu_n^- assuming $\beta = 1.06$ eV and $r_s = 1.41$ Å.²⁴ The HMO results for Cu_2^- and Cu_3^- (0.72 eV and 1.20 eV, respectively) are about 10-15% smaller than the corresponding experimental data, namely

0.79 (3) eV and 1.4 (12) eV, from Ref.17. Table I also gives Hückel electron affinities obtained from Eq.(1) using $EA(1) = 1.24$ eV. The HMO electron affinities are compared with the corresponding experimental values^{16,17} in Figure 2. The agreement between the two data sets is quite good. Both show an odd > even alternation in EA, superimposed on a smoothly increasing classical result.³¹ The occurrence of an odd-even alternation, which also appears in IP data, has a straightforward explanation.^{16,17,21,22} Roughly speaking, an *even* numbered neutral cluster possesses a set of filled bonding orbitals plus an equal number of empty antibonding (AB) orbitals. The IP of such a cluster is (again, roughly speaking) the energy of the highest bonding orbital. *Odd* *n* clusters possess an additional, half filled nonbonding (NB) orbital, lying in between the bonding and AB manifolds. The lower energy of this orbital gives rise to the low IP of an odd atom neutral cluster. For anions, the lowest energy AB orbital is partially filled for *n* even, but is empty for *n* odd. As a consequence, the anion IP's are, in general, lower for even numbered cluster sizes. That there is a reasonable correspondence between this simple orbital picture and the more realistic HMO results is evident from the orbital diagram, Fig. 2 of Ref. 2.

IV. DISCUSSION

Within the framework of the HMO model, at least, there is a tendency for anion clusters to adopt structures which are somewhat less compact²⁰ than those found for the neutrals. One possible cause for this behaviour is the additional kinetic energy (KE) associated with the extra electron of the anions. A close packing arrangement minimizes the potential energy (PE) of a cluster by maximizing the number of bonds between atoms. For *rare gas* clusters, in which the electrons are confined to the atomic cores, this interaction is dominant and so the most compact arrangement of atoms is generally predicted to be the most stable one.³² The stability of a *metal* cluster is determined not only by the pairwise potential interaction between nearest neighbor atoms, but also by the KE of the valence electrons which are delocalized over the molecular framework. In the HMO model, there is a strong correspondence between the energy (E_{1S} , in hu) of the lowest

1s-molecular orbital and $\langle q \rangle$, the average number of bonds (i.e. nearest neighbours) per atom in the cluster. Table III shows some representative examples. Included in this Table are the most stable neutral cluster structures found by HMO calculations in Ref.1, plus some additional geometries ($D_{\infty h}$, T_d for $n = 3$ and 4 ; C_{4v} and D_{5h} for $n = 5$); which compare differing packing arrangements and dimensionalities. For the data of Table II the average difference between E_{1s} and $\langle q \rangle$ is only 2%.

A similar correspondence pertains to macroscopic samples.^{2,24} The 1s level in HMO theory correlates with the $k = 0$ position ($k =$ wavevector) of a metal in the bulk limit.² In the tight binding model, which is the macroscopic counterpart of Hückel theory, the electronic energy of a metal may be expanded near $k = 0$ to give a PE term plus a KE term.^{2,24} The latter is the same as the energy expression obtained from the Fermi gas model for free electrons. The PE (in hu) is numerically identical to the number (6, 8 or 12) of nearest neighbours in a (simple, body centered or face centered) cubic lattice.

Thus for an HMO cluster, the total energy may be considered to be approximately partitioned into two competing components: a negative potential contribution, nearly equal in magnitude to the energy of the 1s level, and a positive KE associated with the delocalized valence electrons. This implies that any stabilization of less compact structures originates in a reduction of the electronic KE, suggesting that more compact structures confine the valence electrons to a smaller volume. This should give rise to larger KE's which would be of relatively greater importance for negatively charged clusters. A similar competition might explain why, for the neutral tetramer and pentamer, the less compact planar structures are predicted²⁻⁶ to be more stable than the three-dimensional arrangements favored by rare gas clusters.

It is straightforward to compute packing fractions for differing, but regular, arrangements of atoms in a macroscopic sample.²⁴ For a cluster composed of *hard* sphere (eg. argon) atoms, then the volume occupied by the electrons is independent of structure. For the case of alkali-like atoms, however, the valence electrons presumably occupy a

volume defined by the shape and bonding arrangement of the individual cluster. This volume was estimated using a *soft* sphere model. Each atom was assigned a unit charge occupying a spherical volume *larger* than the hard sphere volume which determines nearest neighbour distances. The soft sphere radius was chosen as the distance where the electron density for an atomic (for example Na) Slater orbital has fallen to about 90% (say) of its maximum value.³³ The total size of a particular arrangement of n atoms is the volume enclosed by n overlapping soft spheres, and this may be estimated by Monte Carlo integration.³⁴

Some pertinent soft sphere cluster volumes are given in column 5 of Table III. The data pertain to neutral Na clusters, with estimated errors (1 standard deviation uncertainty) given in parentheses and a total of 50,000 integration points except for $n = 2-5$ for which 10^6 points were employed. Cluster volumes are displayed as total volumes, $V(n)$, divided by the volume of n individual atoms. For $n = 6 - 9$, the data correspond to the most stable HMO neutral structures (point group given in column 2) as discussed in Ref. 1. The data for $n = 3, 4$ and 5 compare the soft sphere volumes of clusters having different degrees of compactness. Thus the D_{3h} trimer has an approximately 4% smaller volume than the linear $D_{\infty h}$ arrangement. Similarly, the three-dimensional tetrahedral cluster is approximately 2.5% smaller in total volume than the planar (but more stable²⁻⁶) rhombus. The variation amongst pentamer structures is somewhat greater. The pentagonal arrangement is 5% larger than the most stable²⁻⁶ neutral (C_{2v} point group), and 7.5% larger than the three-dimensional square pyramid (C_{4v} point group).

While small, these differences in soft sphere volumes are both statistically and physically significant. The volume of an n atom cluster is proportional to its classical polarizability, $\alpha(n)$,³⁵ implying

$$\frac{\alpha(n)}{n\alpha(1)} = \frac{V(n)}{nV(1)} \quad (11)$$

Figure 3 compares soft sphere $V(n)/nV(1)$ data from Table III with the experimental polarizabilities for $\text{Na}_2 - \text{Na}_9$.³⁶ The experimental polarizabilities decrease slowly to a bulk value of $\alpha(n)/n\alpha(1) \sim 0.4 - 0.5$, but oscillate about the soft sphere average particularly at small n . These oscillations arise from quantum effects and have been partially accounted for by jellium calculations.^{4,37,38} The soft sphere model does not (of course) include quantum effects and the slight discontinuity at $n \sim 6$ is a manifestation of the transition from two-dimensional to three-dimensional geometries.

Also shown in Fig.3 is a cruder classical approximation:

$$\frac{\alpha(n)}{n\alpha(1)} = \frac{(n^{1/3} + \epsilon^0)^3}{n(1 + \epsilon^0)^3} \quad (12)$$

Eq. (12) assumes that the cluster is a spherical classical drop whose radius is related to an atomic radius (r_0) by

$$r = r_0 (n^{1/3} + \epsilon^0) \quad (13)$$

This expression is similar to Eq. (7), but here ϵ^0 is the "charge spillout" parameter appropriate to a *neutral* cluster. The classical drop curve shown in Fig. 3 pertains to $\epsilon^0 = 0.23$, which was obtained by fitting all the polarizability data ($n = 2 - 40$) in Ref. 36. The agreement between the two classical results is surprisingly good, especially in view of the differing and independent parameterizations for each model and so lends additional authority to the classical drop model invoked in this work and elsewhere.^{2,12,17,36}

In conclusion, we have determined the most stable HMO structures for the alkali-like metal cluster anions, $M_3^- - M_8^-$. The HMO geometries are somewhat less "compact" than those of the neutral and cation clusters, and it is suggested that this may be related to the additional electronic KE of the anions. The cluster compactness is quantified not only by bond enumeration, but also through an estimation of soft sphere volumes, the latter

being directly related to cluster polarizabilities. The Huckel model gives electron affinities which compare favorably with the experimental results for $\text{Cu}_2 - \text{Cu}_8$.

ACKNOWLEDGMENTS

One of us (DML) acknowledges the support of this work by the National Science Foundation under Grants No. CHE 83-07164 and RII 83-05241 and by The City University of New York PSC-BHE Faculty Research Award Program. This work was supported in part by the CRS Program, The City College. TFG acknowledges research support by the Office of Naval Research and the Air Force Office of Scientific Research (AFSC), United States Air Force, under Contract No. F49620-86-C-0009. The United States Government is authorized to reproduce and distribute reprints notwithstanding any copyright notation hereon.

REFERENCES

1. Y. Wang, T. F. George, D. M. Lindsay and A. C. Beri, *J. Chem. Phys.* **86**, 3493 (1987).
2. D. M. Lindsay, Y. Wang, and T. F. George, *J. Chem. Phys.* **86**, 3500 (1987).
3. J. L. Martins, J. Buttet, and R. Car, *Phys. Rev.* **B31**, 1804 (1985).
4. M. Manninen, *Phys. Rev.* **B34**, 6886 (1986).
5. J. Koutecky and P. Fantucci, *Chem. Rev.* **86**, 539 (1986) and references therein.
6. B. K. Rao and P. Jena, *Phys. Rev.* **B23**, 2058 (1985).
7. D. M. Lindsay, D. R. Herschbach and A. L. Kwiram, *Mol. Phys.* **32**, 1199 (1976); G. A. Thompson and D. M. Lindsay, *J. Chem. Phys.* **74**, 959 (1981); D. A. Garland and D. M. Lindsay, *J. Chem. Phys.* **78**, 2813 (1983).
8. G. A. Thompson, F. Tischler and D. M. Lindsay, *J. Chem. Phys.* **78**, 5946 (1983); D. A. Garland and D. M. Lindsay, *J. Chem. Phys.* **80**, 4761 (1984).
9. J. A. Howard, K. F. Preston and B. Mile, *J. Am. Chem. Soc.* **103**, 6226 (1981); J. A. Howard, K. F. Preston, R. Sutcliffe and B. Mile, *J. Phys. Chem.* **87**, 536 (1983); J. A. Howard, R. Sutcliffe and B. Mile, *J. C. S. Chem. Comm.*, 1449 (1983).
10. K. Kernisant, G. A. Thomspson and D. M. Lindsay, *J. Chem. Phys.* **82**, 4739 (1985); D. M. Lindsay, G. A. Thompson and Y. Wang, *J. Phys. Chem.* **91**, XXXX (1987).
11. ESR spectra show that Ag_7 has a pentagonal bipyramidal geometry. See: S. B. H. Bach, D. A. Garland, R. J. Van Zee and W. Weltner, *J. Chem. Phys.* in press.
12. A. Hermann, E. Schumacher and L. Wöste, *J. Chem. Phys.* **68**, 2327 (1978); M. M. Kappes, P. Radi, M. Schär and E. Schumacher, *Chem. Phys. Lett.* **119**, 11 (1985); M. M. Kappes, M. Schär, P. Radi and E. Schumacher, *J. Chem. Phys.* **84**, 1863 (1986).
13. K. I. Peterson, P. D. Dao, R. W. Farley and A. W. Castleman, *J. Chem. Phys.* **80**, 1780 (1984).
14. C. Bréchnac, Ph. Cahuzac and J. Ph. Roux, *Chem. Phys. Lett.* **127**, 445 (1986).
15. W. A. Saunders, K. Clemenger, W. A. de Heer and W. D. Knight, *Phys. Rev.* **B32**, 1366 (1985).
16. L. S. Zheng, C. M. Karner, P. J. Brucat, S. H. Yang, C. L. Pettiette, M. J. Craycraft and R. E. Smalley, *J. Chem. Phys.* **85**, 1681 (1986).
17. D. G. Leopold, J. Ho and W. C. Lineberger, *J. Chem. Phys.* **86**, 1715 (1987).

18. J. L. Gole, R. H. Childs, D. A. Dixon and R. A. Eades, *J. Chem. Phys.* **72**, 6368 (1980); S. C. Richtsmeier, R. A. Eades, D. A. Dixon and J. L. Gole, *Am. Chem. Soc. Symp. Ser.* **179**, 177 (1982).
19. H. Basch, *J. Am. Chem. Soc.* **103**, 4657 (1981).
20. One measure of a structure's compactness is the total number of bonds (q). Thus, for example, the C_{4v} geometry for M_5 with $q = 8$ is significantly more compact than the D_{5h} arrangement for which $q = 5$. A three-dimensional model provides a less objective but more enlightening gauge of compactness. We have found a balloon containing ping-pong balls to be particularly helpful in visualizing cluster shapes. In Section IV, we relate cluster compactness to cluster volume.
21. P. Joyes, *J. Phys. Chem. Solids*, **32**, 1269 (1971).
22. R. C. Baetzold, *J. Chem. Phys.* **55**, 4363 (1971); **68**, 555 (1978).
23. The molecular β values (0.98 eV and 1.01 eV) were obtained by dividing the measured dimer and trimer atomization energies, 1.97 ± 0.06 eV and 3.05 ± 0.13 eV respectively (see Ref. 25), by the corresponding Hückel values. The bulk parameter ($\beta = 1.16$ eV) pertains to the experimental cohesive energy (Ref. 24) divided by the HMO value (see Ref. 2) of 3.00β . A similar analysis gives $\langle\beta\rangle = 0.89 \pm 0.06$ eV for Ag, and $\langle\beta\rangle = 1.23 \pm 0.06$ for Au.
24. C. Kittel, *Introduction to Solid State Physics* (Wiley, New York, 1976).
25. K. Hilpert, *Ber. Bunsenges. Phys. Chem.* **83**, 161 (1979); K. Hilpert and K. A. Gingerich *ibid.* **84**, 739 (1980).
26. J. M. Smith, *AIAA Journal* **3**, 648 (1965).
27. D. W. Wood, *Phys. Rev. Lett.* **46**, 749 (1981).
28. H. B. Michaelson, *J. Appl. Phys.* **48**, 4729 (1977).
29. In Ref. 2 we showed a similar correspondence between $W(\infty) - W(1)$ and $3e^2/8r_s$ for the alkali metals. For the Group IB elements, however, these two parameters can differ by as much as 20%.
30. H. Hotop and W. C. Lineberger, *J. Phys. Chem. Ref. Data* **4**, 539 (1975).
31. Since $|E^-(n)| \leq |E^0(n)|$ for $n = 2 - 8$, the HMO electron affinities all fall below or on a classical curve defined by Eq.(9). The classical IP, by contrast, is more nearly a smooth parameterization of the HMO data (see Ref. 2).

32. For example, see: M. R. Hoare and P. Pal, *Adv. Phys.* **20**, 161 (1971); M. R. Hoare, *Adv. Chem. Phys.* **40**, 49 (1979).
33. In practice we chose a soft sphere radius, $r_c = 0.75$ in units of the nearest-neighbour distance. If the latter is taken to be twice the Wigner-Seitz radius, then for Li \rightarrow Cs the Slater orbital electron density at $r_c = 0.75$ is approximately 10 - 15% of its maximum value.
34. W. H. Press, B. P. Flannery, S. A. Teukolsky and W. T. Vetterling, *Numerical Recipes* (Cambridge, New York, 1986).
35. J. O. Hirschfelder, C. F. Curtiss and R. B. Bird, *Molecular Theory of Gases and Liquids* (Wiley, New York, 1954).
36. W. D. Knight, K. Clemenger, W. A. deHeer and W. A. Saunders, *Phys. Rev.* **B31**, 2539 (1985); W. D. Knight, W. A. deHeer and W. A. Saunders, *Z. Phys.* **D3**, 109 (1986).
37. M. J. Puska, R. M. Nieminen and M. Manninen, *Phys. Rev.* **B31**, 3486 (1985); M. Manninen, R. M. Nieminen and M. J. Puska, *Phys. Rev.* **B33**, 4289 (1986).
38. W. Ekardt, *Phys. Rev. Lett.* **52**, 1925 (1984); W. Ekardt, *Ber. Bunsenges. Phys. Chem.* **88**, 289 (1984).

TABLE I. Hückel binding energies, atomization energies and electron affinities. Data in eV pertain to Cu, using $\beta = 1.06(7)$ eV (see text). Neutral cluster energies from Ref.1.

n	$E^0(n)$	$E^-(n)$	$\Delta E^0(n)/n$	$\Delta E^-(n)/n$	EA(n)
	hu		eV		
1	0.0000	0.0000	0.00	0.00	1.24
2	- 2.0000	- 1.0000	1.06	0.72	0.56
3	- 3.0000	- 2.8284	1.06	1.20	1.65
4	- 5.1231	- 4.1231	1.36	1.28	0.93
5	- 6.6443	- 6.4721	1.41	1.54	1.91
6	- 9.3711	- 8.2005	1.66	1.61	0.95
7	-11.1054	-11.1054	1.68	1.83	2.26
8	-14.1604	-12.7268	1.88	1.82	0.82

TABLE II. Atomic electron affinities, EA(1), bulk work functions, $W(\infty)$, and Wigner-Seitz radii (r_s , in Å) for the Group IA and IB metals. Columns 5 and 6 compare $W(\infty) - EA(1)$ with $5e^2/16r_s$. Energy units are eV.

	EA(1) ^a	$W(\infty)$ ^b	r_s ^c	$W(\infty) - EA(1)$	$4.5/r_s$
Li	0.62	2.32	1.72	1.70	2.62
Na	0.55	2.75	2.08	2.20	2.16
K	0.50	2.30	2.57	1.80	1.75
Rb	0.49	2.09	2.75	1.60	1.64
Cs	0.47	2.14	2.98	1.67	1.51
Cu	1.24	4.65	1.41	3.41	3.19
Ag	1.30	4.26	1.60	2.96	2.81
Au	2.31	5.1	1.59	2.8	2.83

^a From Ref. 30.

^b From Ref. 28.

^c From Ref. 24.

TABLE III. Comparison of the average number of bonds/atom $\langle q \rangle$ with the lowest Hückel orbital energy (E_{1s} in hu), and of soft sphere volume polarizabilities $V(n)$ with the experimental $\alpha(n)$ for Na_n .

n	Point Group	$\langle q \rangle^a$	$ E_{1s} $	$V(n)/nV(1)^b$	$\alpha(n)/n\alpha(1)^c$
2	$D_{\infty h}$	1.00	1.00	0.920	0.800
3	D_{3h}	2.00	2.00	0.862	0.980
3	$D_{\infty h}$	1.33	1.41	0.896	
4	T_d	3.00	3.00	0.814	
4	D_{2h}	2.50	2.56	0.835	0.856
5	C_{4v}	3.20	3.24	0.798	
5	C_{2v}	2.80	2.94	0.819	0.907
5	D_{5h}	2.00	2.00	0.859	
6	C_{5v}	3.33	3.45	0.781	0.857
7	D_{5h}	4.29	4.32	0.742	0.723
8	D_{2d}	4.50	4.54	0.726	0.687
9	D_{3h}	4.67	4.70	0.717	0.738

^a From Ref. 1.

^b Estimated error ± 0.003 for $n = 2 - 5$; ± 0.013 for $n = 6 - 9$.

^c From Ref. 36.

FIGURE CAPTIONS

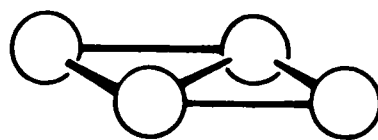
Fig. 1. Geometries for the most stable HMO clusters, M_3^- - M_8^- .

Fig. 2. Comparison of Hückel and experimental electron affinities for Cu^- - Cu_8^- . Open circles pertain to this work. Triangles and full circles are EA data from Refs. 16 and 17, respectively.

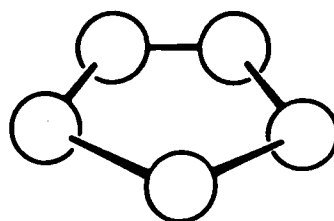
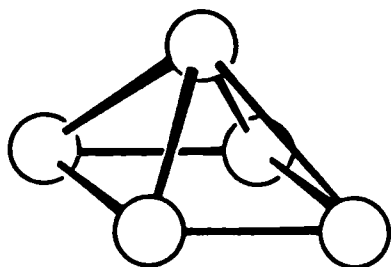
Fig. 3. Comparison of experimental polarizabilities (Na data from Ref. 36) with soft sphere (see text) and classical drop approximations.



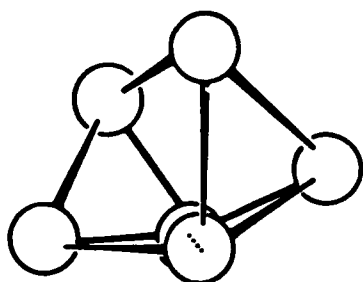
(a). M_3^-



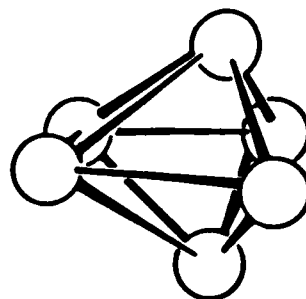
(b). M_4^-



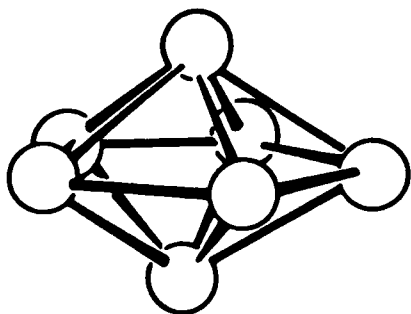
(c). ISOERGIC M_5^- STRUCTURES



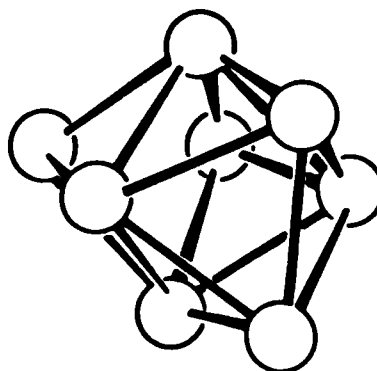
(d). M_6^- (FIRST)



(e). M_6^- (SECOND)



(f). M_7^-



(g). M_8^-

FIG. 1

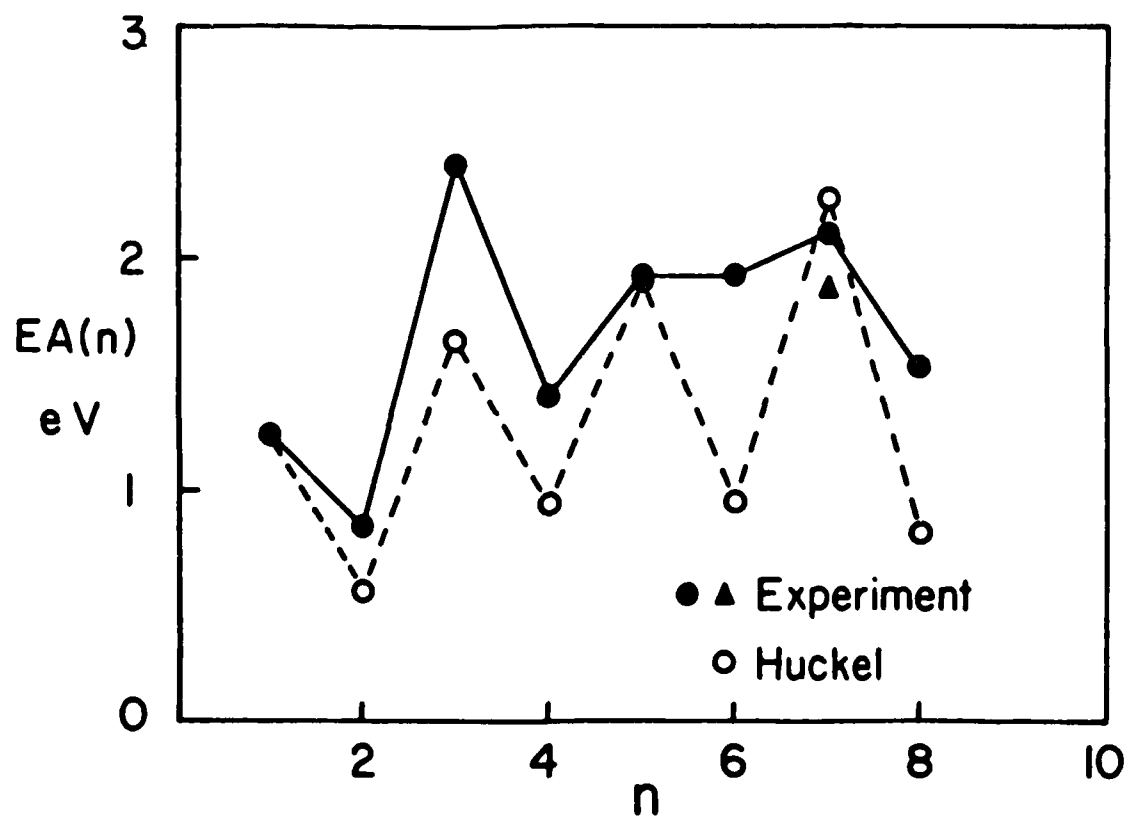


FIG. 2

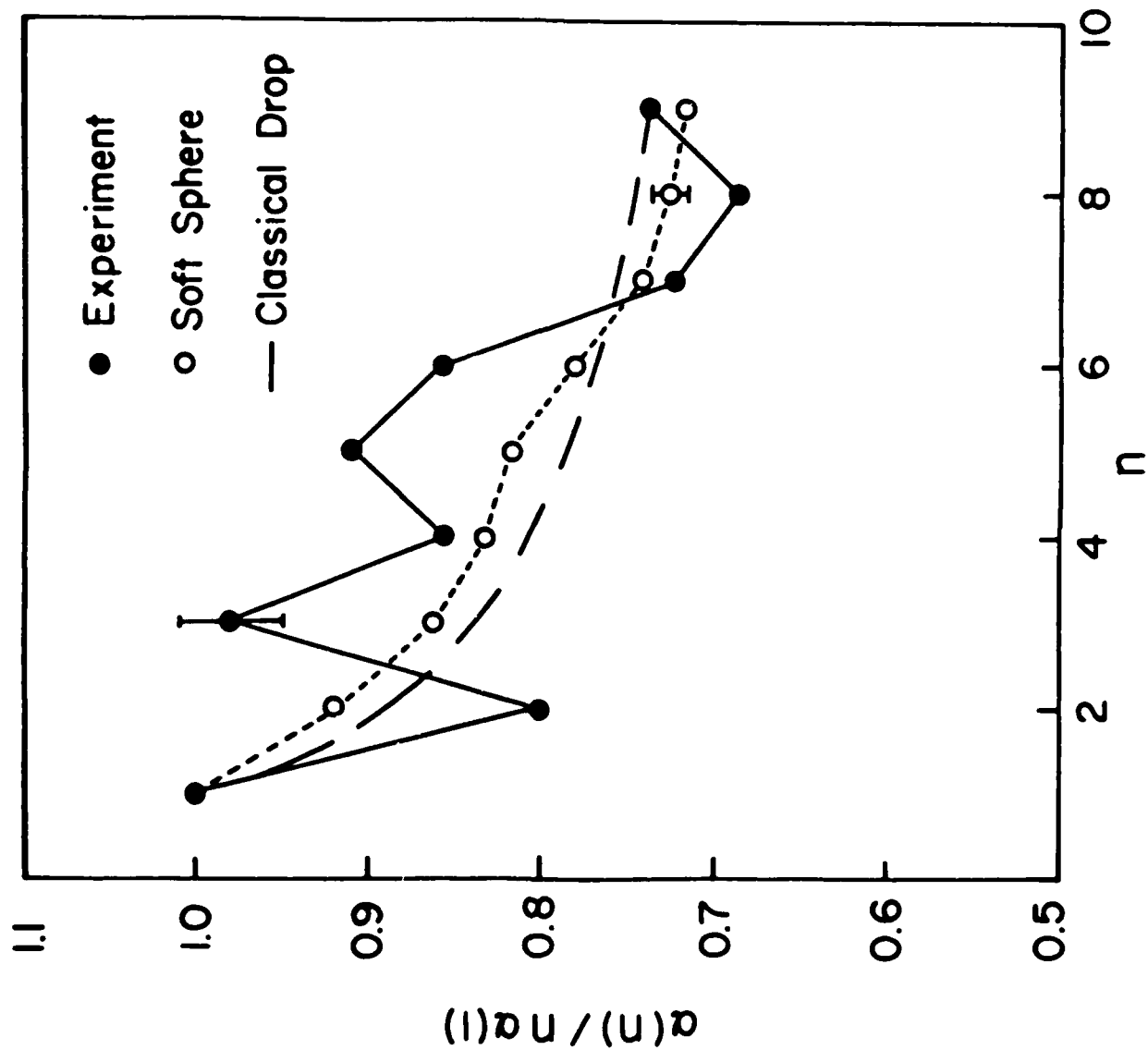


FIG. 3

TECHNICAL REPORT DISTRIBUTION LIST, GEN

	<u>No. Copies</u>		<u>No. Copies</u>
Office of Naval Research Attn: Code 1113 800 N. Quincy Street Arlington, Virginia 22217-5000	2	Dr. David Young Code 334 NORDA NSTL, Mississippi 39529	1
Dr. Bernard Douda Naval Weapons Support Center Code 50C Crane, Indiana 47522-5050	1	Naval Weapons Center Attn: Dr. Ron Atkins Chemistry Division China Lake, California 93555	1
Naval Civil Engineering Laboratory Attn: Dr. R. W. Drisko, Code L52 Port Hueneme, California 93401	1	Scientific Advisor Commandant of the Marine Corps Code RD-1 Washington, D.C. 20380	1
Defense Technical Information Center Building 5, Cameron Station Alexandria, Virginia 22314	12 high quality	U.S. Army Research Office Attn: CRD-AA-IP P.O. Box 12211 Research Triangle Park, NC 27709	1
DTNSRDC Attn: Dr. H. Singerman Applied Chemistry Division Annapolis, Maryland 21401	1	Mr. John Boyle Materials Branch Naval Ship Engineering Center Philadelphia, Pennsylvania 19112	1
Dr. William Tolles Superintendent Chemistry Division, Code 6100 Naval Research Laboratory Washington, D.C. 20375-5000	1	Naval Ocean Systems Center Attn: Dr. S. Yamamoto Marine Sciences Division San Diego, California 91232	1
		Dr. David L. Nelson Chemistry Division Office of Naval Research 800 North Quincy Street Arlington, Virginia 22217	1

ABSTRACTS DISTRIBUTION LIST, 056/625/629

Dr. J. E. Jensen
Hughes Research Laboratory
3011 Malibu Canyon Road
Malibu, California 90265

Dr. C. B. Harris
Department of Chemistry
University of California
Berkeley, California 94720

Dr. J. H. Weaver
Department of Chemical Engineering
and Materials Science
University of Minnesota
Minneapolis, Minnesota 55455

Dr. F. Kutzler
Department of Chemistry
Box 5055
Tennessee Technological University
Cookeville, Tennessee 38501

Dr. A. Reisman
Microelectronics Center of North Carolina
Research Triangle Park, North Carolina
27709

Dr. D. DiLella
Chemistry Department
George Washington University
Washington D.C. 20052

Dr. M. Grunze
Laboratory for Surface Science and
Technology
University of Maine
Orono, Maine 04469

Dr. R. Reeves
Chemistry Department
Rensselaer Polytechnic Institute
Troy, New York 12181

Dr. J. Butler
Naval Research Laboratory
Code 6115
Washington D.C. 20375-5000

Dr. Steven M. George
Stanford University
Department of Chemistry
Stanford, CA 94305

Dr. L. Interante
Chemistry Department
Rensselaer Polytechnic Institute
Troy, New York 12181

Dr. Mark Johnson
Yale University
Department of Chemistry
New Haven, CT 06511-8118

Dr. Irvin Heard
Chemistry and Physics Department
Lincoln University
Lincoln University, Pennsylvania 19352

Dr. W. Knauer
Hughes Research Laboratory
3011 Malibu Canyon Road
Malibu, California 90265

Dr. K.J. Klaubunde
Department of Chemistry
Kansas State University
Manhattan, Kansas 66506

ABSTRACTS DISTRIBUTION LIST, 056/625/629

Dr. G. A. Somorjai
Department of Chemistry
University of California
Berkeley, California 94720

Dr. J. Munday
Naval Research Laboratory
Code 6170
Washington, D.C. 20375-5000

Dr. J. B. Hudson
Materials Division
Rensselaer Polytechnic Institute
Troy, New York 12181

Dr. Theodore E. Madey
Surface Chemistry Section
Department of Commerce
National Bureau of Standards
Washington, D.C. 20234

Dr. J. E. Demuth
IBM Corporation
Thomas J. Watson Research Center
P.O. Box 218
Yorktown Heights, New York 10598

Dr. M. G. Lagally
Department of Metallurgical
and Mining Engineering
University of Wisconsin
Madison, Wisconsin 53706

Dr. R. P. Van Duyne
Chemistry Department
Northwestern University
Evanston, Illinois 60637

Dr. J. M. White
Department of Chemistry
University of Texas
Austin, Texas 78712

Dr. D. E. Harrison
Department of Physics
Naval Postgraduate School
Monterey, California 93940

Dr. R. L. Park
Director, Center of Materials
Research
University of Maryland
College Park, Maryland 20742

Dr. W. T. Peria
Electrical Engineering Department
University of Minnesota
Minneapolis, Minnesota 55455

Dr. Keith H. Johnson
Department of Metallurgy and
Materials Science
Massachusetts Institute of Technology
Cambridge, Massachusetts 02139

Dr. S. Sibener
Department of Chemistry
James Franck Institute
5640 Ellis Avenue
Chicago, Illinois 60637

Dr. Arnold Green
Quantum Surface Dynamics Branch
Code 3817
Naval Weapons Center
China Lake, California 93555

Dr. A. Wold
Department of Chemistry
Brown University
Providence, Rhode Island 02912

Dr. S. L. Bernasek
Department of Chemistry
Princeton University
Princeton, New Jersey 08544

Dr. W. Kohn
Department of Physics
University of California, San Diego
La Jolla, California 92037

ABSTRACTS DISTRIBUTION LIST, 056/625/629

Dr. F. Carter
Code 6170
Naval Research Laboratory
Washington, D.C. 20375-5000

Dr. Richard Colton
Code 6170
Naval Research Laboratory
Washington, D.C. 20375-5000

Dr. Dan Pierce
National Bureau of Standards
Optical Physics Division
Washington, D.C. 20234

Dr. R. Stanley Williams
Department of Chemistry
University of California
Los Angeles, California 90024

Dr. R. P. Messmer
Materials Characterization Lab.
General Electric Company
Schenectady, New York 22217

Dr. Robert Gomer
Department of Chemistry
James Franck Institute
5640 Ellis Avenue
Chicago, Illinois 60637

Dr. Ronald Lee
R301
Naval Surface Weapons Center
White Oak
Silver Spring, Maryland 20910

Dr. Paul Schoen
Code 6190
Naval Research Laboratory
Washington, D.C. 20375-5000

Dr. John T. Yates
Department of Chemistry
University of Pittsburgh
Pittsburgh, Pennsylvania 15260

Dr. Richard Greene
Code 5230
Naval Research Laboratory
Washington, D.C. 20375-5000

Dr. L. Kesmodel
Department of Physics
Indiana University
Bloomington, Indiana 47403

Dr. K. C. Janda
University of Pittsburg
Chemistry Building
Pittsburg, PA 15260

Dr. E. A. Irene
Department of Chemistry
University of North Carolina
Chapel Hill, North Carolina 27514

Dr. Adam Heller
Bell Laboratories
Murray Hill, New Jersey 07974

Dr. Martin Fleischmann
Department of Chemistry
University of Southampton
Southampton SO9 5NH
UNITED KINGDOM

Dr. H. Tachikawa
Chemistry Department
Jackson State University
Jackson, Mississippi 39217

Dr. John W. Wilkins
Cornell University
Laboratory of Atomic and
Solid State Physics
Ithaca, New York 14853

ABSTRACTS DISTRIBUTION LIST, 056/625/629

Dr. R. G. Wallis
Department of Physics
University of California
Irvine, California 92664

Dr. D. Ramaker
Chemistry Department
George Washington University
Washington, D.C. 20052

Dr. J. C. Hemminger
Chemistry Department
University of California
Irvine, California 92717

Dr. T. F. George
Chemistry Department
University of Rochester
Rochester, New York 14627

Dr. G. Rubloff
IBM
Thomas J. Watson Research Center
P.O. Box 218
Yorktown Heights, New York 10598

Dr. Moria Metiu
Chemistry Department
University of California
Santa Barbara, California 93106

Dr. W. Goddard
Department of Chemistry and Chemical
Engineering
California Institute of Technology
Pasadena, California 91125

Dr. P. Hansma
Department of Physics
University of California
Santa Barbara, California 93106

Dr. J. Baldeschwieler
Department of Chemistry and
Chemical Engineering
California Institute of Technology
Pasadena, California 91125

Dr. J. T. Keiser
Department of Chemistry
University of Richmond
Richmond, Virginia 23173

Dr. R. W. Plummer
Department of Physics
University of Pennsylvania
Philadelphia, Pennsylvania 19104

Dr. E. Yeager
Department of Chemistry
Case Western Reserve University
Cleveland, Ohio 44106

Dr. M. Winograd
Department of Chemistry
Pennsylvania State University
University Park, Pennsylvania 16802

Dr. Roald Hoffmann
Department of Chemistry
Cornell University
Ithaca, New York 14853

Dr. A. Stecki
Department of Electrical and
Systems Engineering
Rensselaer Polytechnic Institute
Troy, New York 12181

Dr. G.H. Morrison
Department of Chemistry
Cornell University
Ithaca, New York 14853

END

6-87

DITIC